Pt(100) quasihexagonal reconstruction: A comparison between scanning tunneling microscopy data and effective medium theory simulation calculations

G. Ritz, M. Schmid, and P. Varga
Institut für Allgemeine Physik, Technische Universität Wien, A-1040 Wien, Austria

A. Borg
Department of Physics, The Norwegian University of Science and Technology, N-7034 Trondheim, Norway

M. Rønning
Department of Industrial Chemistry, The Norwegian University of Science and Technology, N-7034 Trondheim, Norway

(Received 31 October 1996; revised manuscript received 25 April 1997)

The interpretation of scanning tunneling microscopy (STM) data is usually limited to first-layer effects, but with increasing resolution of the STM images deeper-layer effects may also become visible in the top-layer corrugations. We have investigated the clean Pt(100) surface, which is known to be pseudohexagonally reconstructed and for which there is some evidence for a second-layer reconstruction. The big unit cell makes it difficult to investigate the deeper layers by traditional methods like low-energy-electron diffraction (LEED). We have, therefore, used a ''fingerprint'' technique to compare highly resolved STM data of the clean Pt(100) surface to effective-medium-theory simulation calculations in order to determine the geometric structure of the second atomic layer. We were able to show that STM can be sensitive to deeper layer effects and that excellent agreement could only be achieved for an unreconstructed second layer. The simulation results also agree well with the corrugations determined by LEED whereas the maximum corrugation amplitude is higher than previously derived from helium-diffraction measurements. [S0163-1829(97)05739-1]

I. INTRODUCTION

In recent years scanning tunneling microscopy (STM) has evolved into one of the most powerful techniques for investigating surface structures. Because of the imaging process, real-space pictures of the surface on an atomic scale can be obtained. Therefore STM could often identify the surface unit cell where scattering or diffraction techniques could not yield conclusive results. However, the interpretation of the atomic corrugations obtained by STM is usually limited to effects in the first layer, because only the positions of the uppermost atoms are directly accessible. But with increasing resolution of the STM images, effects of deeper layers may be visible in highly resolved images under certain circumstances.[1–4] In this case the interpretation of the STM data is not easy, if at all possible, without accompanying simulation calculations. Such a system with a heavily reconstructed first layer, which may also be at least partly reconstructed in the subsurface layer, is the Pt(100) surface, which has been investigated by means of low-energy-electron diffraction[5–8] (LEED) and other techniques[9–14] for many years. But only recently, a STM study[15] gave the first highly resolved real-space picture of this reconstruction. The reconstructed Pt(100) surface, which is similar to the Ir and Au (100) surfaces, is not cubic, but rather has a hexagonal symmetry. Whereas the (1×5) superstructure cell of Ir(100) is relatively small, the unit cells of Pt(100) and Au(100) are much larger. For the Pt(100) surface, two hexagonal phases have been reported: the Pt(100)-hex and the Pt(100)-hex-$R0.7°$ reconstructions.[5,14] Upon gas exposure (CO, NO, O_2, and C_2H_4) the reconstruction can be lifted and the surface transforms into a (1×1) structure.[13,15,16] The formation and lifting of the reconstruction is also supposed to play an important role in catalytic reactions.[16]

There are several indications that the second atomic layer may also be reconstructed.

(1) The analysis of Rutherford backscattering measurements in Ref. 9 leads to the conclusion that approximately 10% of the second layer atoms must be displaced more than 0.01 nm. It is clear, however, from these measurements that the second layer is not, like the first layer, completely hexagonally reconstructed. Only some atoms in the second layer can be in positions out of registry with the bulk atoms.

(2) The comparison of an *ab initio* calculation[17] and the measurement[18] of the energy gain of the reconstruction, which result in ≈0.0 eV and 0.21 eV per (1×1) unit cell, respectively, leads to a considerable discrepancy. Since the calculation in Ref. 17 is based on an unreconstructed second layer, this may also point towards a reconstruction of the second layer.

(3) The analysis of LEED I/V data for Ir(100),[19] which has a structure similar to Pt(100), only gave a Pendry R factor of $R_P=0.62$. This could be caused by the presence of a reconstruction in the second layer that has not been assumed in the study in Ref. 19.

Unfortunately, the unit cell of the Pt(100)-hex reconstruction is too big for LEED and no experimental method can give a real-space picture of the second atomic layer. But by comparing results from computer simulations with the corrugation in the STM pictures, one can try to obtain information about the second layer.

In this paper we will present effective-medium-theory (EMT) computer calculations for the Pt(100)-hex surface. The simulation results will be compared to high-resolution

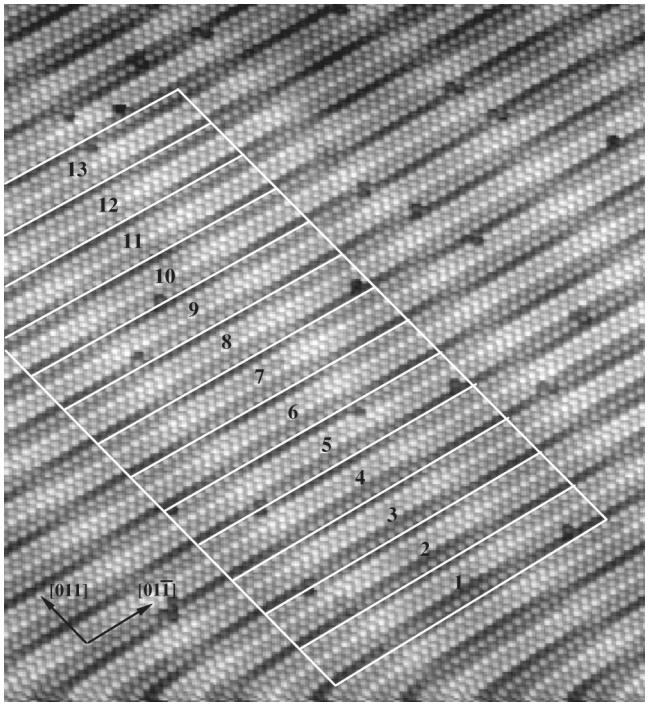

FIG. 1. Large STM scan of the unrotated hexagonally reconstructed Pt(100) surface. The image size is 200 Å×200 Å. 13 cells of (6×30) surface atoms are marked. The reconstruction unit cell is slightly smaller than six surface atom distances in the [011] direction, so the cell becomes shifted in the [011] direction with respect to the cubic substrate, which yields a modulation of the corrugation pattern inside the (6×30) cell. From this modulation the periodicity of the superstructure can be estimated.

STM images and the structure of Ir(100) determined by LEED.[19] We further compare the maximum corrugation amplitude in the STM images and the EMT calculations to the value derived from helium-diffraction measurements.[20]

II. STM RESULTS

In their STM study of Pt(100), Borg, Hilmen, and Bergene[15] presented high-quality atomically resolved pictures of the reconstructed Pt(100) surface. The STM image (Fig. 1) shows the unrotated Pt(100)-hex structure. The superstructure cell extends over 30 atoms in [011] and 6 atoms in the [011] direction, which can be seen even better in Fig. 2. However, there is a long-range modulation visible in the [011] direction, which indicates that the reconstructed surface layer does not have an exactly fivefold periodicity: In cell *A* in Fig. 2(a) the corrugation is approximately symmetrical in the [011] direction around the row with the brighter atoms (row 4). The schematic detail in Fig. 2(c) illustrates this symmetry. In cell *B*, however, the atoms in the rows adjacent to row 4 (rows 3 and 5) clearly do not have the same brightness, as is indicated by the schematic detail in Fig. 2(b). The atoms in row 3 are darker than the atoms in row 5. The height difference between row 3 and row 5 is approximately 0.3 Å. Besides, there is in addition to row 4, a second row with brighter atoms (row 6). Between cells *A* and *B* row 6 is gradually becoming brighter. This long-range modulation can be explained by a surface unit cell with a size in the [011] direction that is slightly different from the length of five nearest-neighbor distances of the fcc bulk. In this case the (29×5) unit cell becomes shifted by a small

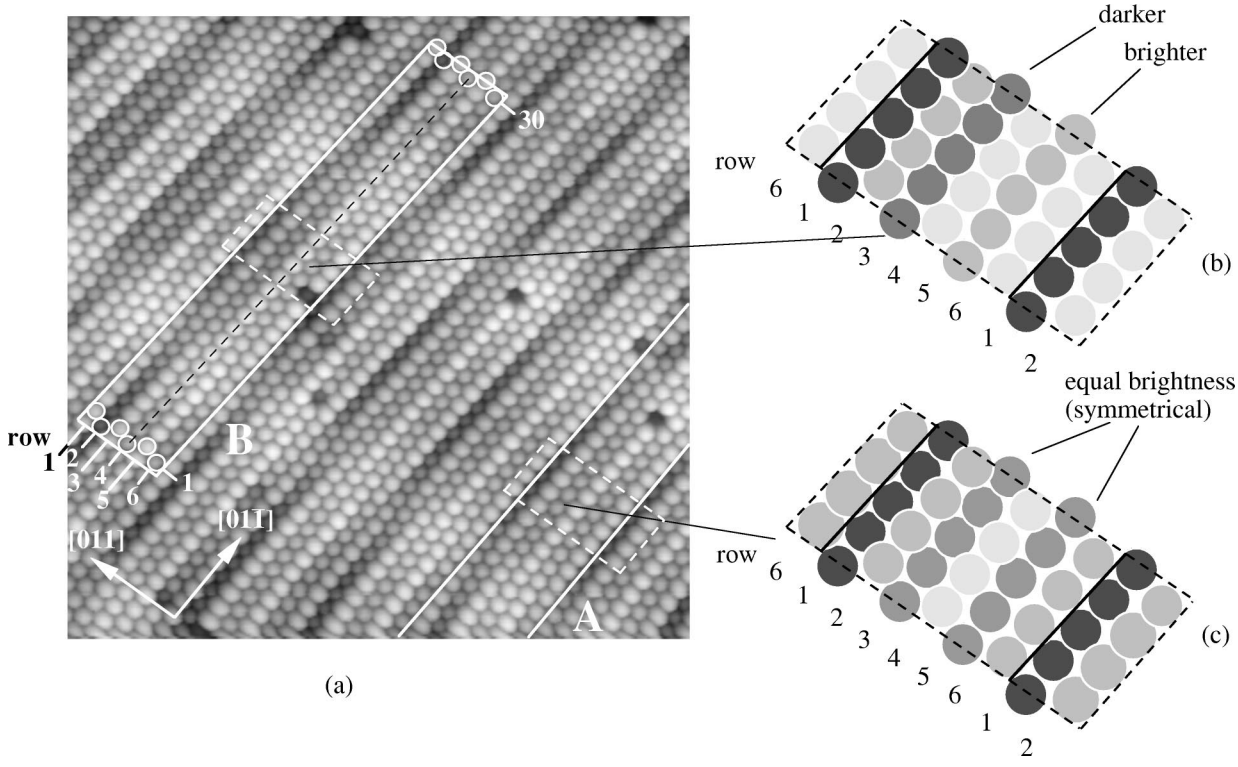

FIG. 2. (a) STM image of the hexagonally reconstructed Pt(100) surface (Ref. 15). Two unit cells (*A* and *B*) of the reconstruction are shown (cell *A* is only partly visible). The image size is 100 Å×100 Å. (b) Schematic detail of the area within the dashed lines in cell *B*. The rows adjacent to row 4 (rows 3 and 5) have different brightnesses. (c) Schematic detail of the corresponding area in cell *A*. The corrugation is symmetrical around row 4, i.e., rows 3 and 5 and rows 2 and 6 have the same brightness, respectively.

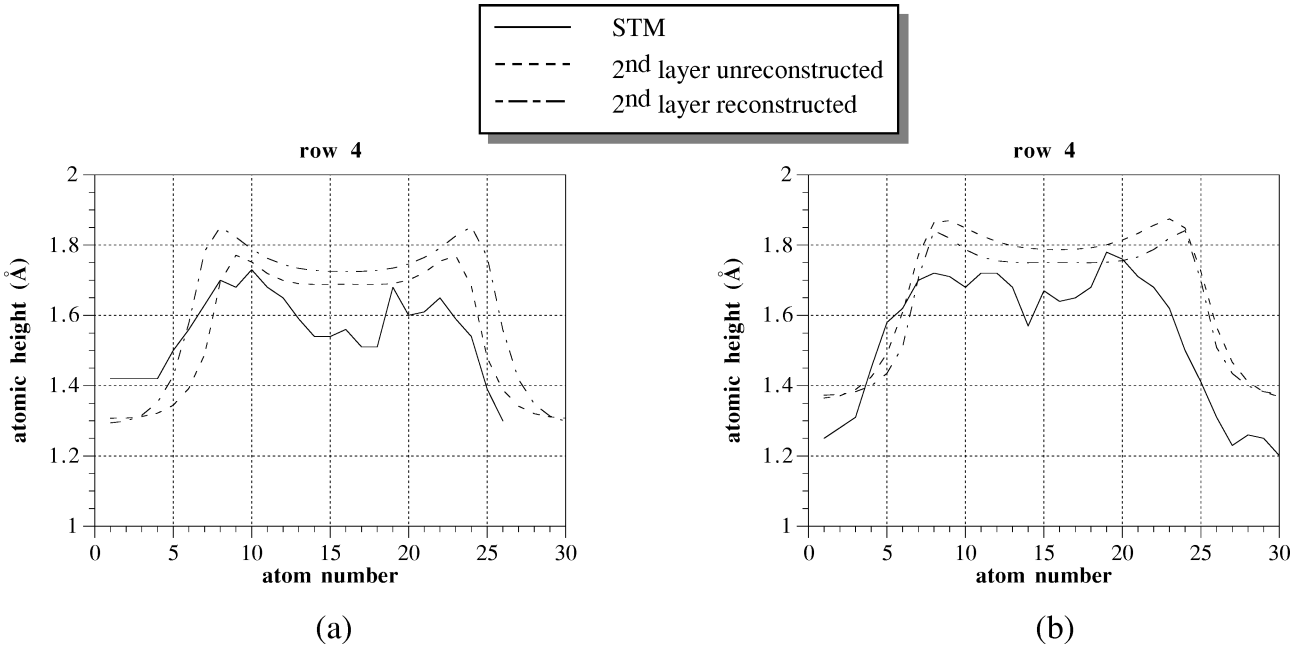

FIG. 3. Line scans (solid lines) along row 4 in the STM image [Fig. 2 (a)] for (a) the symmetrical cell, which is in registry with the second layer (cell *A*) and (b) for the unsymmetrical cell, which is displaced in the [011] direction (cell *B*). A slight depression is seen in the center of the cell, where on-top positions would be expected for the surface atoms. The difference between the minimum in the center of the cell (atom 14) and the maximum (atom 19) is approximately 0.1–0.2 Å. The dashed and the dash-dotted curves show the calculated line scans for the two cells with an unreconstructed and a reconstructed second layer, respectively.

amount in the [011] direction out of registry with the cubic second layer with each period and, therefore, changes its corrugation pattern. In other words, the structure is not exactly described by the (29×5) unit cell but is rather either very large in the [011] direction, as is also suggested in Ref. 21, or incommensurate. The modulation of the corrugation can also be seen in the larger STM scan in Fig. 1. From this modulation the periodicity of the superstructure in the [011] direction can be estimated: The symmetric cell in the lower right edge of the image (marked 1) is chosen as the starting point of the periodicity. The symmetric cell on the top left edge (marked 13) represents the center of the period in the [011] direction (there are only two possible symmetric first-layer configurations with the Pt(100)-hex reconstruction: one on the edge of the large-range unit cell and one in the middle with a shift of a half of a row distance in the [011] direction). The whole period therefore is approximately 26 cells of (29×5) size or 156 surface atoms on 129 substrate atoms. The cell size of 129 is in reasonable agreement with the proposed cell size of 150 in Ref. 21 for the unrotated phase.

The STM images show another interesting feature, which is revealed by the line scan over row 4 in Fig. 2 (see Fig. 3). Starting from the edge of the cell where the atoms in row 4 occupy bridge sites, as can be seen from section I in the schematic picture in Fig. 4(a), the atomic heights increase. The maximum height, however, is not reached in the center of the (29×5) cell, where the first-layer atom in row 4 should be located exactly on top of the atom in the second layer [section II in Fig. 4(a)], which would yield the maximum height in a hard-sphere model assuming an unreconstructed second layer, but rather halfway between the center and the edge of the cell. Between the two maxima the atomic heights slightly decrease, which is rather unexpected. The amount of this depression in the STM image depends on the cell considered, but is in the range of 0.1–0.2 Å. This corrugation could be seen as a fingerprint of a local reconstruction of the second layer below the atoms in the center of the (29×5) cell, which would avoid the energetically disfavored on-top positions.

In order to investigate this feature in the STM image more closely, we determined the first layer corrugations for different second-layer configurations by use of simulation calculations.

III. SIMULATION METHOD

For a complete simulation of the measured STM corrugation it would be necessary to calculate the local density of states (LDOS) around the Fermi level in a distance of a few angstroms above the surface[22] and possibly its derivatives[23] with an *ab initio* method, as the STM really samples the electronic structure rather than the topography of the surface. Nevertheless, the STM corrugation has repeatedly and successfully been interpreted as geometric information about the surface.[2,4] For pure metals this can be explained by the similar environment an individual atom on the surface experiences, which yields only minor differences in the electronic structure of the atoms at different positions. The corrugation amplitude above an atom is thus related to its atomic position as the decay of the density of states into the vacuum region is approximately equal for all surface atoms. A difference of the LDOS at the Fermi level of, e.g., 10% would only yield a corrugation difference of about 5 pm, which is small compared to the measured corrugation of up to 100 pm.

In addition to that, a simulation with an *ab initio* method of a (29×5) unit cell with a hexagonally reconstructed first layer, a possibly reconstructed second layer, and a few bulk layers would require enormous computational effort that cur-

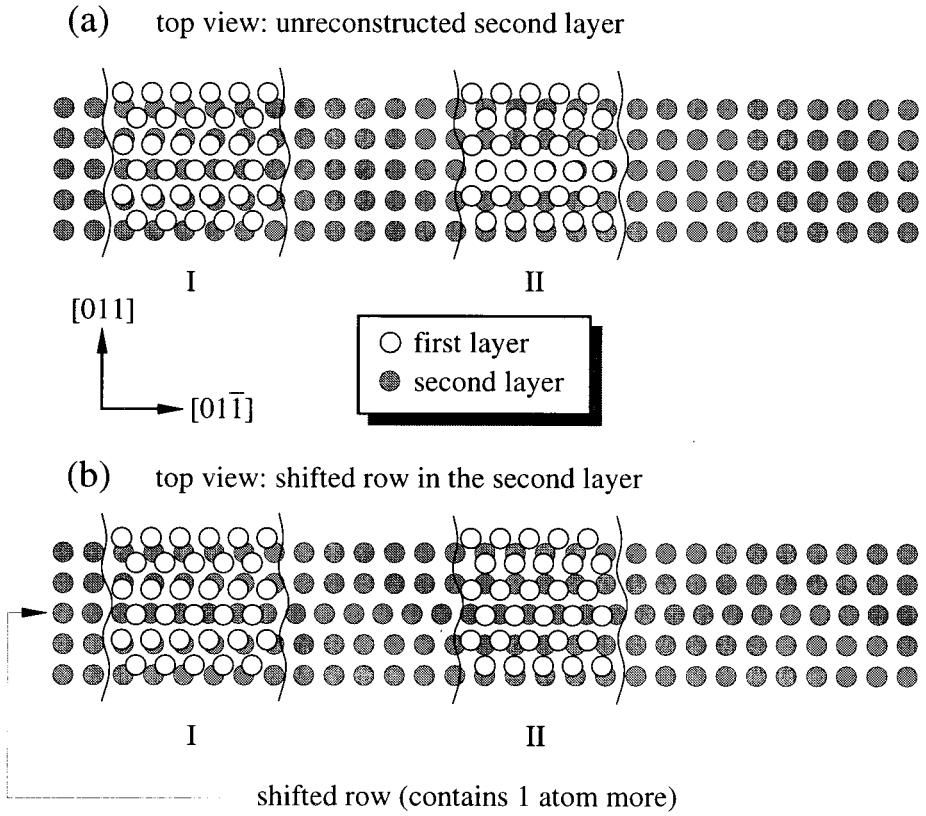

FIG. 4. Top view of the first two layers of the crystal configurations used for the simulations. For clarity, the first layer is only shown in two sections (labeled I and II), one at the edge of the unit cell and one near the center. (a) Configuration with unreconstructed second layer. The first layer atoms in the center of the cell are located exactly above the atoms in the second layer. (b) Configuration with a shifted row in the second layer. The first-layer atoms in the center of the cell now occupy bridge sites, which should yield a smaller atomic height of the first-layer atoms in this region with respect to the unreconstructed configuration. The shifted row contains one atom more.

rent computers cannot handle. We therefore have used a faster, so-called semiempirical method, which describes the energy of a crystal with only a few parameters fitted to experimental and/or *ab initio* calculated data. Instead of calculating the LDOS corrugation above the surface, we compute the atomic positions of the surface atoms and compare the corrugation of the core positions to the measured STM corrugation. As stated above, because we investigate a pure metal surface with approximately equally coordinated surface atoms, the STM corrugation should be mainly determined by the atomic positions.

Out of the semiempirical potentials available, EMT is among the methods closest to *ab initio* calculations, since both the method itself and some of its parameters are based on density-functional theory.[24,25] The effective-medium theory has been employed successfully for many metallic systems and is described in several papers.[24–27] The simulations have been performed with the ARTWORK computer code developed at the Technical University of Denmark with potentials given in Ref. 27. For calculating the atomic positions a molecular-dynamics energy minimization routine has been used. The simulations have been performed in a slab geometry with periodic boundary conditions in the two surface directions. The slabs consisted of 10 layers with 5×29 atoms per layer, except for the topmost layer, which had a hexagonal structure and, therefore, consisted of 6×30 atoms. The atomic positions in the bottom two layers have been fixed to bulk positions whereas the upper surface has been allowed to relax in the direction perpendicular to the surface and partly in the in-surface directions.

The calculation of the first-layer corrugations for the Pt(100)-hex reconstruction is somewhat tricky, as a simulation crystal having initially a hexagonal surface tries to deconstruct because with the EMT potentials used the unreconstructed surface has a lower energy. For a cell consisting of 10 layers and 5 atoms per layer, the calculated energy of the unreconstructed surface is 0.68 eV lower than the energy for the same cell with a perfect 5×1 hexagonally reconstructed surface. This is not surprising, since EMT generally underestimates the surface energies and, hence, also the energy gain coming from the difference between close packed and more open surfaces. But this is not a specific problem for this technique or the potentials used. The instability of the hexagonal reconstruction is quite insensitive to the exact parameters. Also, other popular potentials used for metals such as the embedded-atom-method potentials (both those published by Foiles[28] and Voter *et al.*[29]) suffer from the same problem.

It has to be mentioned, however, that even the *ab initio* calculations in Ref. 17 yield a slightly lower energy for the unreconstructed (100) surface. It is therefore necessary to artificially stabilize the hexagonal first layer, which would, however, make a comparison of the calculated energies for an unreconstructed and a reconstructed second layer rather meaningless. To avoid this problem we will use a kind of

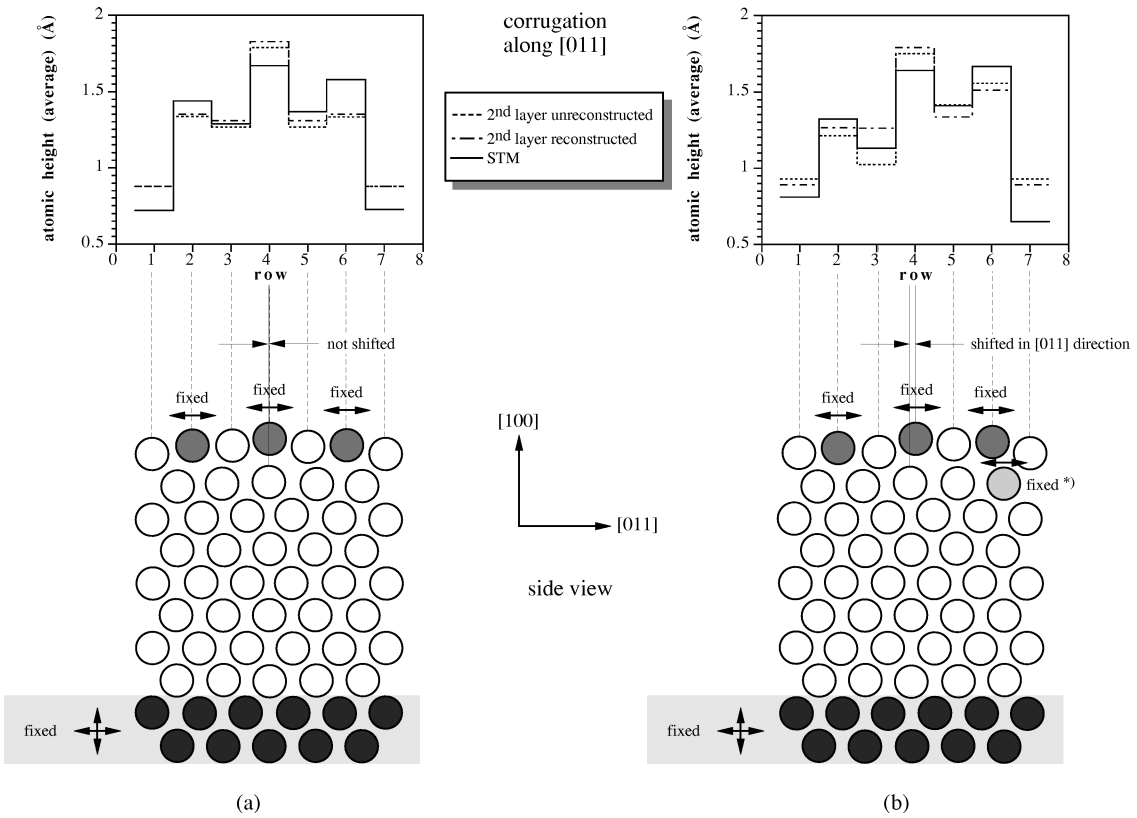

FIG. 5. Side view (bottom) and corrugation (top) of the first layer in the [011] direction of the simulation results. The atomic positions in the rows marked in gray have been fixed in the direction(s) given by the arrows for stabilizing the first-layer reconstruction. The atomic heights have been averaged over five atoms and the corrugation in the STM image is also given for comparison. (a) Configurations (with and without reconstructed second layer) with unshifted first layer (corresponds to cell *A* in Fig. 2). The corrugation is symmetrical around row 4 in both configurations and quite comparable with the STM data. (b) The first layer is shifted in [011] direction (corresponds to cell *B* in Fig. 2). The row in the second layer marked in light gray has been fixed in the [011] direction only in the configuration with a reconstructed second layer to avoid shear of the crystal. The corrugation of the configuration with a shifted row in the second layer is rather symmetrical around row 4, whereas both the STM corrugation and the corrugation of the configuration with an unreconstructed second layer are clearly unsymmetrical, i.e., the height of row 3 is approximately 0.4 Å lower than the height of row 5.

fingerprint technique by comparing the calculated atomic positions, i.e., the calculated corrugation, for selected crystal configurations with the corrugation in the STM images. The effective-medium theory has already proven to yield reliable atomic corrugations (see Refs. 2 and 4).

To avoid transformation to the (1×1) phase the movement of the atoms in the first two layers had to be restricted in critical areas. In Fig. 5 the rows where the atomic positions have been fixed in the [011] direction are marked in gray. In the other directions the atoms have been free to move. Since such constraints can severely influence the behavior of the system care has been taken, so that the atoms had enough freedom for arranging without destroying the reconstruction, e.g., by fixing only those atomic coordinates given by the symmetry of the reconstructed cell.

IV. SIMULATION CONFIGURATIONS

As already mentioned it is not possible to determine the atomic arrangement in the second layer by simply comparing the calculated energies of different crystal configurations. We instead use an indirect way by comparing the atomic corrugation of the first layer in the computer simulations with the measured corrugation in the STM image. By choosing characteristic simulation configurations it should be possible to determine from this comparison which one of the simulation models is more likely. For the simulations we considered two principal cases.

(i) No reconstruction in the second layer. Only the first layer is hexagonally reconstructed, all other layers are cubic. The configuration used for the simulation is shown in Fig. 4(a).

(ii) The second layer is reconstructed. However, which reconstruction should be assumed? Rutherford backscattering spectroscopy (RBS) measurements[9] show that only a small part of the second layer can be reconstructed. It is clear that a reconstruction would try to avoid the energetically disfavored on-top positions in the first layer. This could be accomplished by shifting some second-layer atoms in the center of the unit cell in the $[0\bar{1}1]$ direction and adding an atom there [see Fig. 4(b)]. Similar *shifted rows* have been observed on the PtNi(100) surface and are suspected to be a precursor to the hexagonal reconstruction.[30] The formerly on-top atoms would then occupy bridge sites and, therefore, are supposed to have a lower height.

To take into account the long range modulation of the corrugation in the [011] direction, which is due to the slight misfit of the quasihexagonal structure with respect to the

cubic substrate, we used two modifications of the simulation crystals described above.

(a) First layer in registry with second layer: The middle row of the top layer is located exactly above the middle row of the second layer, as can be seen from the lower part of Fig. 5(a). This corresponds to cell *A* in the STM image in Fig. 2.

(b) First layer displaced in the [011] direction: The middle row of the first layer is displaced by a tenth of a nearest-neighbor distance in the [011] direction, as can be seen from the lower part of Fig. 5(b). This is the maximum displacement to be considered, because further displacement would only lead to an analogous configuration. The configuration corresponds approximately to cell *B* in the STM image in Fig. 2.

V. SIMULATION RESULTS

We have performed molecular dynamics calculations with all four crystal configurations described in Sec. IV. The final configurations of the molecular-dynamics simulation runs are shown in Fig. 6 in form of ''artificial STM images,'' i.e., the heights of the atoms in the first layer are given by their brightness. As can easily be seen, all four configurations look very similar to each other and to the STM image. However, there are some features that are somewhat different between the four configurations.

A. First layer in registry with second layer (cell *A*)

If we compare the two configurations (with and without a shifted row in the second layer), where row 4 in the first layer is exactly above the row in the second layer [see Fig. 5(a)], there are no obvious differences. The calculated first layer corrugations shown in Figs. 6(a) and 6(b) look almost identical and both are very similar to cell *A* in the STM image in Fig. 2. Of course, the atomic corrugations (averaged over five atoms in the center of the cell) in Fig. 5(a) are symmetrical around row 4 in both configurations (with and without the shifted row in the second layer).

The line scans in Fig. 3 over row 4 for these two configurations both show the slight depression in the center of the unit cell, similar to the STM data, although, in the case of the unreconstructed second layer, the first-layer atoms in the middle of row 4 are located on-top of the atoms in the second layer. This is caused by the second-layer atoms moving inwards in this area. The height differences between the highest atoms and the atoms in the center of the cell are 0.08 Å and 0.13 Å for the configuration without and with a shifted row in the second layer, respectively, which is quite comparable to the experimentally determined value of 0.1–0.2 Å.

B. First layer displaced in [011] direction (cell *B*)

The two configurations shown in Figs. 6(c) and 6(d) where the first layer is displaced in [011] direction [see Fig. 5(b)] differ in one characteristic feature: with a shifted row in the second layer, the corresponding atoms in the rows adjacent to row 4 (rows 3 and 5) have approximately the same height, i.e., the configuration is approximately symmetrical, as can be seen from the calculated corrugation in Fig. 5(b). However, the configuration without a shifted row, i.e., the configuration with no reconstruction in the second layer, is quite unsymmetrical: the atoms left and right of row 4 have a height difference of about 0.4 Å. This feature can also be seen in the STM image in cell *B* and in the cross section through the STM corrugation shown in Fig. 5(b). As in cell *A*, the line scans over row 4 in Fig. 3 show the decrease of atomic heights in the center of the cell in both simulation configurations.

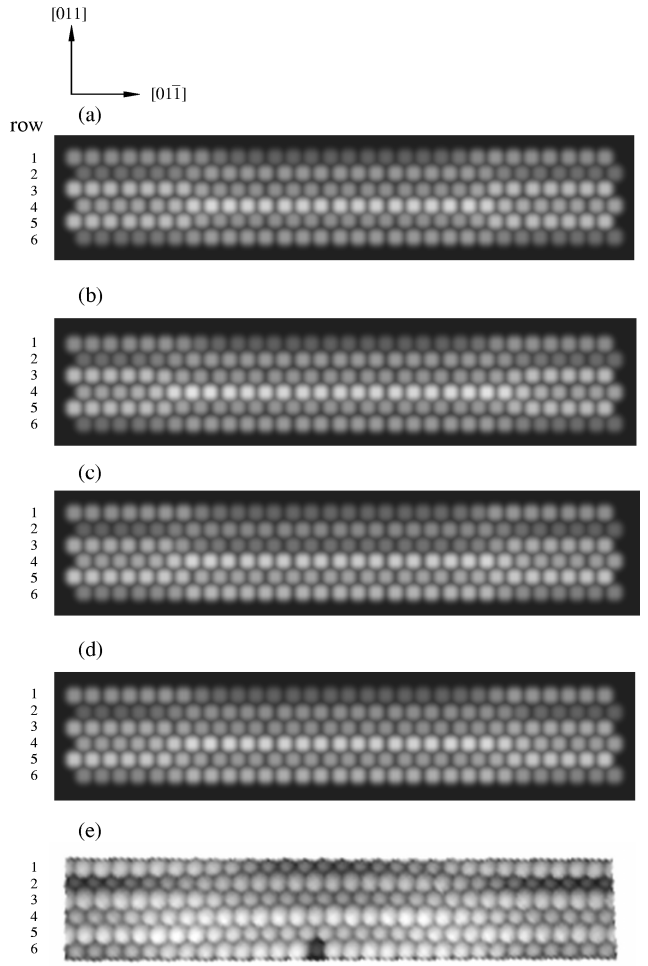

FIG. 6. Results of the EMT computer simulations. The gray-scale corresponds to height. (a) First layer in registry, second layer unreconstructed. (b) First layer in registry, second layer with shifted row. (c) First layer displaced in [011] direction, second layer unreconstructed. (d) First layer displaced in [011] direction, second layer with shifted row. (e) Cell *B* of STM image Fig. 2, corresponding to the configurations with a displaced first layer (c),(d).

VI. DISCUSSION

A. Is the second layer reconstructed?

From the results of the calculations for the configurations where the first layer is in registry with the second layer (corresponding to cell *A* in the STM image in Fig. 2) it is not possible to conclude whether there is a reconstruction in the second layer or not. However, the unsymmetric corrugation, which has been found in the STM image in cell *B*, is correctly reproduced only by the simulation results for the configuration with a displaced first layer and an unreconstructed

second layer. The configuration with a shifted row in the second layer yielded a rather symmetrical corrugation, since the first-layer atoms snap into the bridge sites above the shifted row and cannot freely float on the second layer anymore.

Furthermore, the line scans over row 4 show the decrease of atomic heights, which was mentioned as a possible fingerprint of a second-layer reconstruction, in all four configurations (with and without a reconstructed second layer). This feature in the STM image would, therefore, have been misinterpreted without the simulation calculations because in a simple hard-sphere model one cannot correctly take into account relaxations of the second layer. These relaxations causing the *on-top* atoms in the first layer to have a smaller height must be seen as similar to the inverse corrugation found in overlayers of atoms larger than the substrate.[2,28,31] Thus, a reconstruction of the second layer is not necessary to explain this feature found in the STM image.

One argument for a reconstruction in the second layer came from Rutherford backscattering data in Ref. 9, which indicate that in the pseudohexagonal reconstruction $(1.65\pm0.05)\times10^{15}$ Pt atoms per cm^2 were displaced more than 0.01 nm, which is higher than the areal density of both the bulk Pt(100) plane (1.28×10^{15} Pt atoms per cm^2) and the hexagonal Pt(111) surface (1.5×10^{15} Pt atoms per cm^2) and, thus, lead to the conclusion that approximately 10% of the atoms in the second layer could also be displaced. However, the distance of the $[0\bar{1}1]$ oriented rows of the Pt(100)-hex reconstruction determined from the STM image is $0.821\times$ the row distance of the cubic (100) surface and the rows are also contracted 3.3% in $[01\bar{1}]$ direction. Therefore, the surface areal density of the Pt(100)-hex reconstruction is $1/(0.821\times0.967)\times1.28\times10^{15}=1.61\times10^{15}$ Pt atoms per cm^2 and, thus, within the error bar of the measurements. A reconstruction of the second layer is therefore not necessary to explain the RBS data.

The overall good agreement of the atomic positions in the simulations with the corrugation in the STM image justifies the stabilizing of the hexagonal reconstruction by restricting the movement of the atoms in critical rows to a plane perpendicular to the surface and shows that, in this case, the STM indeed gives topographic information. It has to be noted, however, that the corrugation in the simulation depends on which rows of atoms are exposed to the constraint. If the entire first layer is restricted to relaxation only in the direction perpendicular to the surface, the depression in the line scan over row 4 in Fig. 3 drops from 0.08 Å to approximately 0.05 Å in the case of an unreconstructed second layer. We have used the configurations in Fig. 5 because the rows adjacent to row 4 were free to move and, thus, resulted in a relaxation towards row 4, yielding a higher corrugation. Fewer constrained rows led to a destruction of the hexagonal reconstruction during the simulation run, except for the configuration with a shifted row in the second layer, which remained stable.

It is for the above reasons that we think that a reconstruction in the second layer is unlikely. Although the effective-medium theory is, due to the wrong energetics, not able to give insight into the driving force for the reconstruction (and, therefore, also for the reason why the second layer does not reconstruct) it does give corrugation values in good agreement with the experimental results. A comparison of first layer corrugations calculated by EMT with STM data therefore makes an investigation of deeper-layer effects possible. The problem of different calculated (Ref. 17) and measured (Ref. 18) reconstruction energies remains unresolved, however.

TABLE I. Structural parameters for Pt(100) determined by EMT computer simulations compared to Ir(100) LEED results of Ref. 5.

	Pt(100) (EMT)	Ir(100) (LEED)
ΔZ_1 (Å)	0.62	0.5
ΔZ_2 (Å)	0.20	0.28
d_{12} (Å)	1.91–2.12	1.975

[a]Reference 5.

B. Comparison with LEED and helium diffraction

Unfortunately, there are no quantitative LEED data available for the atomic corrugations of the large Pt(100)-hex unit cell. However, at the edge of the unit cell the hexagonal Pt(100) reconstruction has a two-bridge configuration equivalent to that found in a LEED study of the pseudohexagonal Ir(100) (1×5) surface.[19] We therefore compare the calculated atomic positions at the edge of the Pt(100)-hex unit cell to LEED results on Ir(100).

Table I gives the structural parameters extracted from the EMT simulation together with the optimal parameters of the Ir(100) LEED study in Ref. 19. The meaning of the parameters can be seen from the schematic view in Fig. 7. The quite good agreement of the calculated corrugations with the structural parameters for Ir(100) determined by LEED indicates that the simulation procedure used yields reasonable results.

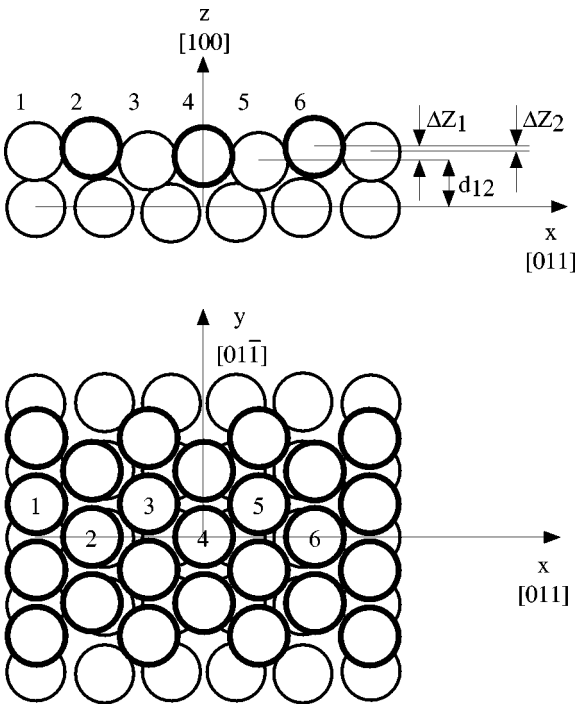

FIG. 7. Structural parameters listed in Table I.

The maximum corrugation amplitude [i.e., the height difference between the highest and lowest atom in the (29×5) unit cell] of 1.2 Å in the STM image is in good agreement with the value of 1 Å determined from the EMT simulation calculations. These values are, however, considerably higher then the corrugation amplitude of 0.5–0.75 Å for the rotated Pt(100)-hex-$R0.7°$ structure derived from helium-diffraction measurements.[20]

VII. CONCLUSIONS

We have determined the reconstruction unit cell of the quasihexagonal Pt(100) reconstruction from STM data. We have found that the corrugation pattern in the (29×5) unit cells changes with subsequent cells in the [011] direction resulting in either an incommensurate structure or a very large unit cell in the [011] direction with a period of approximately 129 substrate atoms, which is in reasonable agreement with the unit size of 150 atoms determined by high-resolution helium diffraction.[21] The Pt-Pt distance in the first layer is contracted 3.3% with respect to the bulk. We have further found that the atoms, which should be in on-top positions, have a slightly smaller height than their neighbors, which could be caused by a reconstruction of the second layer. However, our EMT simulations showed that the calculated corrugation for an unreconstructed second layer is in good agreement with the STM data, whereas the configurations with a shifted row in the second layer did not show the unsymmetric corrugation found in the STM image. This comparison of calculated (in our case by EMT) first-layer corrugations and the STM data can thus be used to gain information about the second atomic layer. In the case of the Pt(100) surface we conclude from our calculations that a reconstruction of the second layer is unlikely. We have also shown that the calculated corrugation is in good agreement with the structural parameters of Ir(100) determined by LEED but is higher than previous helium diffraction and STM measurements have indicated.

ACKNOWLEDGMENTS

We are very grateful to P. Stoltze, K. W. Jacobsen, and J. K. Nørskov for supplying us with the EMT computer code. This work was supported by the ''Fonds zur Förderung der Wissenschaftlichen Forschung'' (Austrian Science Foundation) under Project No. S6201. A.B. and M.R. acknowledge the financial support from the Norwegian Research Council.

[1] M. Schmid, W. Hebenstreit, P. Varga, and S. Crampin, Phys. Rev. Lett. **76**, 2298 (1996).
[2] C. Nagl, M. Schmid, and P. Varga, Surf. Sci. **369**, 159 (1996).
[3] M. Schmid, A. Biedermann, H. Stadler, and P. Varga, Phys. Rev. Lett. **69**, 925 (1992).
[4] J. Jacobsen, L. Pleth Nielsen, F. Besenbacher, I. Stensgaard, E. Lægsgaard, T. Rasmussen, K. W. Jacobsen, and J. K. Nørskov, Phys. Rev. Lett. **75**, 489 (1995).
[5] P. Heilmann, K. Heinz, and K. Müller, Surf. Sci. **83**, 487 (1979).
[6] M. A. Van Hove, R. J. Koestner, P. C. Stair, J. P. Bibérian, L. L. Kesmodel, I. Bartoš, and G. A. Smorojai, Surf. Sci. **103**, 189 (1981).
[7] K. Heinz, E. Lang, K. Strauss , and K. Müller, Appl. Surf. Sci. **11/12**, 611 (1982).
[8] K. Heinz, E. Lang, K. Strauss, and K. Müller, Surf. Sci. **120**, L401 (1982).
[9] P. R. Norton, J. A. Davies, D. K. Creber, C. W. Sitter, and T. E. Jackman, Surf. Sci. **108**, 205 (1981).
[10] W. Hösler, E. Ritter, and R. J. Behm, Ber. Bunsenges. Phys. Chem. **90**, 205 (1986).
[11] W. Hösler, R. J. Behm, and E. Ritter, IBM J. Res. Dev. **30**, 403 (1986).
[12] R. J. Behm, W. Hösler, E. Ritter, and G. Binnig, Phys. Rev. Lett. **56**, 228 (1986).
[13] E. Ritter, R. J. Behm, G. Pötschke, and J. Wintterlin, Surf. Sci. **181**, 403 (1987).
[14] D. L. Abernathy, S. G. J. Mochrie, D. M. Zehner, G. Grübel, and Doon Gibbs, Phys. Rev. B **45**, 9272 (1992).
[15] A. Borg, A.-M. Hilmen, and E. Bergene, Surf. Sci. **306**, 10 (1994).
[16] M. P. Cox, G. Ertl, and R. Imbihl, Phys. Rev. Lett. **54**, 1725 (1985).
[17] V. Fiorentini, M. Methfessel, and M. Scheffler, Phys. Rev. Lett. **71**, 1051 (1993).
[18] Y. Y. Teo, C. E. Wartnaby, and D. A. King, Science **268**, 1731 (1995).
[19] N. Bickel and K. Heinz, Surf. Sci. **163**, 435 (1985).
[20] X.-C. Guo, A. Hopkinson, J. M. Bradley, and D. A. King, Surf. Sci. **278**, 263 (1992).
[21] Klaus Kuhnke, Klaus Kern, and George Comsa, Phys. Rev. B **45**, 14 388 (1992).
[22] J. Tersoff and D. R. Hamann, Phys. Rev. Lett. **50**, 1998 (1983); Phys. Rev. B **31**, 805 (1985).
[23] C. Julian Chen, Phys. Rev. Lett. **65**, 448 (1990); *Introduction to Scanning Tunneling Microscopy* (Oxford University Press, New York, 1993).
[24] K. W. Jacobsen, J. K. Nørskov, and M. J. Puska, Phys. Rev. B **35**, 7423 (1987).
[25] K. W. Jacobsen, Comments Condens. Matter Phys. **14**, 129 (1988).
[26] J. N. Nørskov, K. W. Jacobsen, Pl. Stoltze, and L. B. Hansen, Surf. Sci. **283**, 277 (1993).
[27] P. Stoltze, J. Phys.: Condens. Matter **6**, 9495 (1994).
[28] S. M. Foiles, Surf. Sci. **292**, 5 (1993).
[29] A. F. Voter, S. P. Chen, R. C. Albert, A. M. Boring, and P. J. Hay, in *Atomistic Simulation of Materials—Beyond Pair Potentials*, edited by V. Vitek and D. J. Srolovitz (Plenum, New York, 1989), p. 223.
[30] M. Schmid, A. Biedermann, S. D. Böhmig, P. Weigand, and P. Varga, Surf. Sci. **318**, 289 (1994).
[31] C. Mottet, G. Tréglia, and B. Legrand, Phys. Rev. B **46**, 16 018 (1992).